AIP Applied Physics Letters

Monolithic fabrication of quasi phase-matched waveguides by femtosecond laser structuring the χ (2) nonlinearity

Sebastian Kroesen, Kemal Tekce, Jörg Imbrock, and Cornelia Denz

Citation: Applied Physics Letters **107**, 101109 (2015); doi: 10.1063/1.4930834
View online: http://dx.doi.org/10.1063/1.4930834
View Table of Contents: http://scitation.aip.org/content/aip/journal/apl/107/10?ver=pdfcov
Published by the AIP Publishing

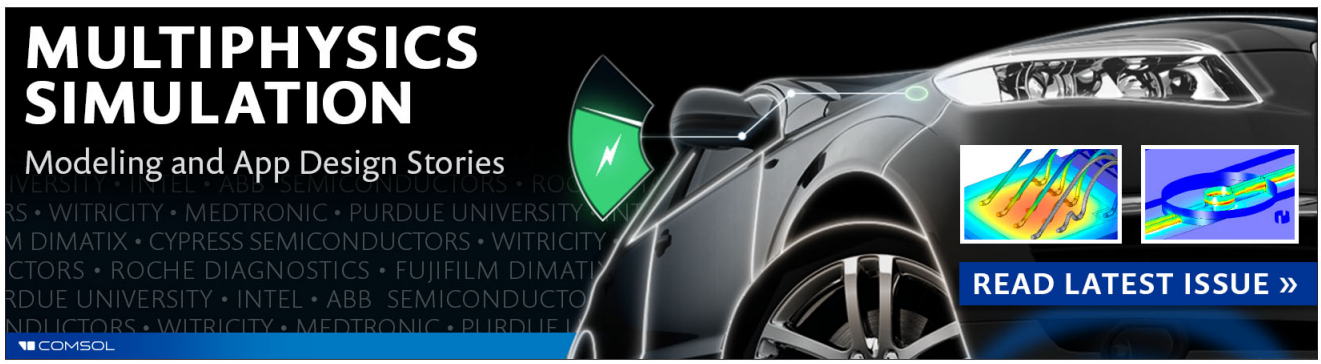

Monolithic fabrication of quasi phase-matched waveguides by femtosecond laser structuring the $\chi^{(2)}$ nonlinearity

Sebastian Kroesen,[a] Kemal Tekce, Jörg Imbrock, and Cornelia Denz
Institute of Applied Physics and Center for Nonlinear Science (CeNoS), University of Muenster, Corrensstr. 2/4, 48149 Muenster, Germany

(Received 9 July 2015; accepted 30 August 2015; published online 11 September 2015)

We demonstrate second harmonic generation in quasi phase-matched waveguide structures fabricated by direct laser writing. Circular waveguides are inscribed in z-cut lithium niobate that provide well confined guiding of the fundamental and second harmonic wave. In contrast to classic schemes that employ periodically poled crystals, quasi phase-matching is realized by a laser-induced modulation of the nonlinearity inside the waveguide core. The proposed design allows monolithic integration of buried frequency conversion devices with tailored nonlinear response and excellent compatibility to on-chip optical elements. Second harmonic generation of 1064 nm radiation is demonstrated for different grating periods and associated matching temperatures. A maximum conversion efficiency of 5.72% is obtained for a 6 mm long, laser-induced quasi phase-matching grating. © *2015 AIP Publishing LLC*.
[http://dx.doi.org/10.1063/1.4930834]

Frequency conversion is one of the most important nonlinear optical processes which is of tremendous significance not only for fundamental research but also for a multitude of industrial products. In particular, second harmonic generation (SHG) in non-centrosymmetric materials has many applications including compact single frequency sources,[1,2] cascaded $\chi^{(2)}$ processes,[3,4] and quantum optical devices.[5–7] The ferroelectric crystal lithium niobate ($LiNbO_3$) is one of the most prominent materials for many of these applications due to its excellent second-order nonlinear properties and large transmission window.[8]

It is well known that the SHG process requires the phase-mismatch $\Delta k = 2\omega(n_{2\omega} - n_\omega)/c$ to be compensated, which can be either achieved by utilizing the intrinsic birefringence of the crystal or by quasi phase-matching (QPM), where the direction of ferroelectric domains is periodically modulated.[9,10] The latter case exhibits the huge advantage that the significantly larger diagonal components of the nonlinear optical tensor ($d_{33} \approx 28 \times 10^{-12}\,\mathrm{m\,V^{-1}}$) can be addressed. Moreover, quasi phase-matching is also applicable whenever the material's dispersion does not allow SHG at the desired wavelength or temperature.

Particularly for efficient frequency conversion at moderate power or continuous wave operation, high intensities are required over a long interaction length which makes waveguides an ideal working platform. Various lithographic methods are well established to create such high quality channel waveguides in periodically poled lithium niobate (PPLN), e.g., in-diffusion or ion implantation. In addition to these standard fabrication techniques, direct laser writing has emerged as a powerful tool for photonic integration and fabrication of complex three-dimensional refractive index structures in various materials including glasses, ceramics, and crystals.[11–13] The technique has been applied to realize waveguide SHG by birefringent phase-matching[14] and quasi phase-matching,[15–17] using different waveguide geometries. However, direct inscription of high fidelity waveguides with symmetric guiding properties in lithium niobate is challenging due to the intrinsic anisotropy. Most recently, multi-line geometries such as *circular* or *depressed cladding* waveguides have been proposed that provide significantly improved extraordinary polarized guiding, which is essential to access features based on the d_{33} coefficient of lithium niobate.[13,18,19] Applying such complex waveguide structures is the first step towards efficient integrated frequency conversion devices.

Lately, Thomas *et al*. reported that the second essential step to realize waveguide SHG devices, the actual material modification that allows quasi phase-matching, can also be addressed by direct laser writing.[20] Instead of domain inversion, the nonlinearity is damped within the coherence length $l_c = \pi/\Delta k$, which reduces out of phase contributions of the SHG process. The effective nonlinear coefficient d_{eff} for a modulation depth (or visibility) $v = d_{\min}/d_{\max}$ is given by

$$d_{\mathrm{eff}} = \frac{d_{\max}}{\pi}(1 - v). \tag{1}$$

It is evident that the efficiency of such a laser-induced quasi phase-matching structure (LiQPM) is below that of a poled one and strongly depends on the modulation depth. The localized reduction of the nonlinear coefficients due to femtosecond material processing is a typical and actually in many cases undesired effect.[21,22] However, in terms of LiQPM structures, it allows to fabricate nonlinear quasi phase-matched waveguides in a single monolithic process. The huge flexibility of direct laser writing enables three-dimensional packaging of multi-wavelength LiQPM devices while providing immediate compatibility to integrated optical elements. Moreover, the LiQPM grating structure and SHG process can be tailored to fulfill demands of next generation nonlinear photonic devices.

[a]Electronic mail: s.kroesen@uni-muenster.de

In this letter, we report on the first experimental realization of laser-induced quasi phase-matched waveguides in lithium niobate by direct femtosecond laser writing. The realized device represents a synthesis of high fidelity, two-dimensional waveguides and localized $\chi^{(2)}$ modifications to access nonlinear functionality. We demonstrate second harmonic generation with different QPM periods and narrow temperature acceptance.

We use a standard direct laser writing configuration to fabricate the LiQPM waveguides as illustrated in Fig. 1(a). The experimental system is based on a Ti:sapphire femtosecond laser with a repetition rate of 1 kHz, up to 1 mJ pulse energy and a pulse duration of 120 fs. To enable position-synchronized pulse firing, which is required for the multiscan grating section, the output is externally modulated using a large aperture Pockels cell.[23] All structures are fabricated at an absolute depth of 100 μm below the surface of the substrate using a 100× microscope objective with a numerical aperture of NA = 0.8. The incident writing beam is polarized parallel to the waveguide direction. We use congruent magnesium doped $LiNbO_3$ for all presented experiments (5.5 mol. %). The individual samples with the dimensions $12 \times 10.5 \times 0.5\,mm^3$ are cut from a z-cut wafer and subsequently polished at a 5° angle to achieve efficient coupling while minimizing undesired Fresnel reflections.

A microscope image of a cladding waveguide with circular cross section based on type-II modifications that is inscribed with a pulse energy of 150 nJ and 80 $\mu m\ s^{-1}$ translation velocity is shown in Fig. 1(b). We found that waveguides with a diameter (or clear aperture) of 10 μm to 15 μm and a line spacing of 2.5 μm exhibit extraordinary polarized single mode guiding at the fundamental wavelength (1064 nm) and reasonably good guiding properties at the second harmonic frequency. A more general discussion on guiding characteristics and anisotropy of two-dimensional waveguide structures can be found for instance in Ref. 19. The LiQPM grating is inscribed using lower pulse energies of 60 nJ to 72 nJ (measured at the sample position), which is associated with a narrow threshold process of starting type-II filamentation. A microscope image of the LiQPM section with a phase-matching period of $\Lambda = 2l_c = 6.7\,\mu m$ is shown in Fig. 1(c), where the upper and lower lines are omitted for clear illustration. The grating is inscribed applying the multiscan technique with high transverse resolution of 700 nm in both directions and 80 $\mu m\ s^{-1}$ translation velocity. In contrast to volume raster scans, the grating region is unidirectionally scanned, and the writing laser beam is unlocked within the coherence length by the positioning electronics. Full inscription sequences are performed in a bottom-up scheme to reduce focus distortion, and fabrication duration of a single LiQPM waveguide is of the order of 150 min according to the large number of successive scans.

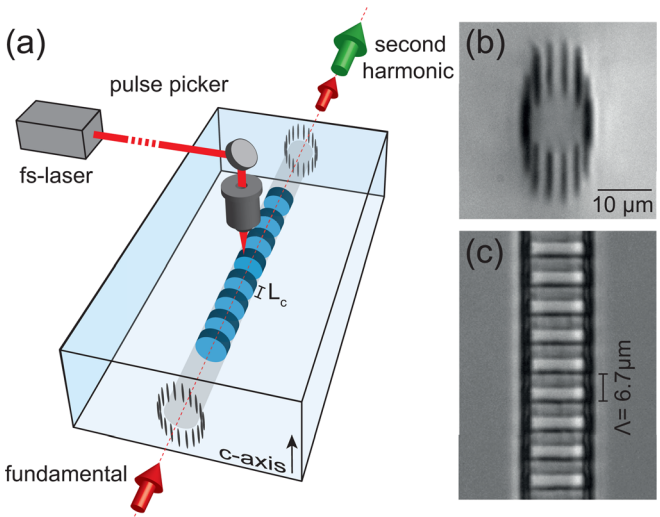

FIG. 1. Schematic of the LiQPM waveguide design in z-cut lithium niobate (a). Optical microscope images the circular waveguide structure (b) and top-view of the multiscan grating section with a period of $\Lambda = 6.7\,\mu m$ (c).

SHG experiments are performed using an optically pumped Nd:YAG laser with a pulse duration of 4.1 ns and a repetition rate up to 100 Hz. According to the probe laser system, the notation *power* within this manuscript refers to the peak power. The processed sample is mounted on a heater element to adjust the phase-matching temperature and probed by free-space coupling using a 5× microscope objective.

Figure 2(a) shows the experimental temperature tuning of a laser-induced quasi phase-matching waveguide. The structure consists of a circular, 9.3 mm long waveguide with a diameter of 12 μm and a 6 mm long embedded grating with a period of 6.7 μm. The grating is inscribed with a pulse energy of 69 nJ, while the waveguide parameters are the same as described in the previous paragraph. A maximum second harmonic power of 20.6 W is obtained for an incident fundamental power of 390 W and extraordinary polarization (s). The temperature acceptance bandwidth of approximately 3.52 °C is in very good agreement with the numerical calculation as shown by the gray solid line. A detailed description of the numerical formalism and related parameters will be given in the next paragraph. It should be noted that the SHG signal shifts by approximately −43 °C with respect to the calculated dispersion curve.[24] This shift corresponds to a

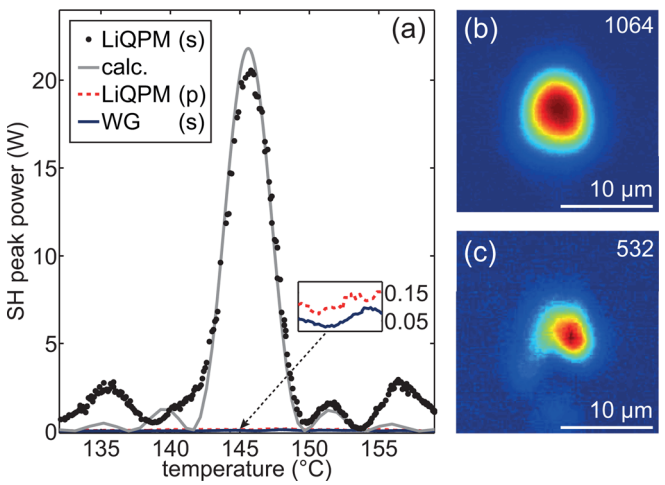

FIG. 2. Experimental temperature tuning of a 9.3 mm long LiQPM waveguide with a 6 mm long embedded grating at 390 W input power (a) and associated numerical calculation. Reference tuning curves are obtained for ordinary input polarization and for a pure waveguide probed with extraordinary polarized light. Corresponding near field mode images of the fundamental (b) and second harmonic wave (c) at the phase-matching temperature $T = 145.7\,°C$.

change of the bulk material's dispersion of $|n_{2\omega} - n_{\omega}| = 9.5 \times 10^{-4}$ due to the refractive index profile of the waveguide. To distinguish from non-critical birefringent phase-matching (oo-e process in 90° geometry), which is around 115 °C, the red dashed line shows the tuning curve obtained for ordinary input polarization (p). It can be clearly seen that the oo-e process does not contribute to the SHG signal. Additionally, we show the extraordinary polarized tuning curve for a pristine reference waveguide (blue solid line) to determine the absolute enhancement factor of the SHG process induced by the LiQPM grating, which is approximately 200 for the given grating strength.

The corresponding near-field mode profiles at the phase-matching temperature $T = 145.7\,^{\circ}\mathrm{C}$ are shown in Figs. 2(b) and 2(c). Pure single mode transmission without any noticeable disturbance due to the LiQPM grating section is observed for the fundamental wave. The full width half maximum at 1064 nm is 5.79 μm in horizontal and 6.79 μm in vertical direction, respectively. According to the refractive index profile of the waveguide at each wavelength, the second harmonic wave is slightly elliptic with the dimensions 5.03 μm and 4.55 μm. Both modes are well confined and show a good spatial overlap. We determine an average propagation loss of $\alpha_{\omega} = 8.33\,\mathrm{dB\,cm^{-1}}$ for the fundamental and $\alpha_{2\omega} = 13.3\,\mathrm{dB\,cm^{-1}}$ for the second harmonic wave using a calibrated (linear) fiber-coupling setup. It should be mentioned that the absolute power transmission at the fundamental wavelength, and thus the SHG process significantly increases for larger waveguides with a diameter of 15 μm to 20 μm. However, in this case, the second harmonic wave shows clearly multimode behavior, and the temperature spectra become impure due to different effective mode indices and related phase-matching conditions.

The second harmonic generation process can be described by a set of coupled mode equations as follows:

$$\frac{dA_{\omega}}{dz} = -i\kappa^{*} A_{\omega}^{*} A_{2\omega} \exp(-i\Delta k z) - \alpha_{\omega} A_{\omega}, \tag{2}$$

$$\frac{dA_{2\omega}}{dz} = -i\kappa A_{\omega}^{2} \exp(i\Delta k z) - \alpha_{2\omega} A_{2\omega}, \tag{3}$$

where A_i denote the amplitudes, z is the propagation coordinate, Δk is the phase mismatch, and α_i is the propagation loss coefficient.[16] The coupling coefficient

$$\kappa^{2} = \frac{2\omega^{2}}{\epsilon_0 c^{3}} \frac{d_{\mathrm{eff}}^{2}}{n_{\omega}^{2} n_{2\omega} S_{\mathrm{eff}}}, \tag{4}$$

depends on the effective nonlinear coefficient d_{eff}, the refractive indices n_i, and the spatial overlap integral of the modes S_{eff}, which can be calculated from the mode profiles. We numerically solved the coupled mode equations to determine the effective nonlinear coefficient d_{eff} and thus the modulation depth of the nonlinear susceptibility.

Figure 3 shows the power of the SH wave at 532 nm and the conversion efficiency of the SHG process as a function of the incident fundamental power. The corresponding numerical calculation considering propagation losses is given by the red solid line. The characteristic quadratic dependency of the second harmonic power $P_{2\omega} \propto P_{\omega}^{2} l^{2}$ and the

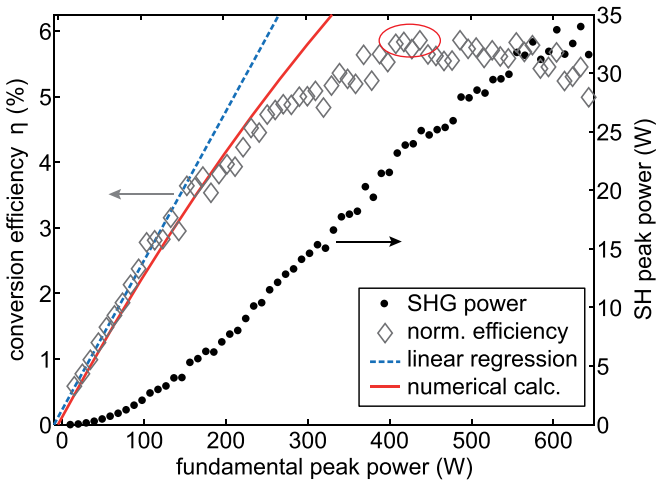

FIG. 3. SH power and conversion efficiency versus input power at the phase-matching temperature and associated numerical calculation with modulation depth of $v = 0.85$. A normalized conversion efficiency of $0.0637\,\%\,\mathrm{W^{-1}\,cm^{-2}}$ is obtained as indicated by the linear regression.

linear slope of the efficiency are clearly observed. A maximum conversion efficiency of $\eta_{\max} = 5.72\,\%$ (red ellipse) and 25.1 W second harmonic power is achieved for an incident fundamental power of 438.5 W. The SHG conversion efficiency increases linearly up to 3.4% and saturates for pump powers larger than 450 W. This saturation effect is not correctly mapped by the numerical calculation and would suggest higher propagation losses in combination with a larger effective nonlinearity. Since the linear propagation losses have been precisely determined, we attribute this behavior to intensity dependent derogation of either the waveguide or LiQPM properties that might be caused by inhomogeneities and defects induced by the femtosecond material processing. The normalized conversion efficiency with respect to the grating length $\eta_{norm} = 0.0637\,\%\,\mathrm{W^{-1}\,cm^{-2}}$ in the undepleted pump regime is determined by the linear regression (blue dashed line). Since different normalization schemes are common, we want to state that only Fresnel reflections are considered and the reference fundamental wave is measured behind the 5× microscope objective. Hence, the unknown coupling efficiency is neglected in all performed calculations.

Based on the experimental data, we estimate an effective nonlinear coefficient of $d_{\mathrm{eff}} = 1.36 \times 10^{-12}\,\mathrm{m\,V^{-1}}$, which corresponds to a modulation depth of approximately $v = 0.85$. This low modulation depth explains the relatively weak conversion in direct comparison to commercially available PPLN waveguides where the d_{33} nonlinear coefficient is addressed which results in $d_{\mathrm{eff}} = 2/\pi d_{33}$ ($\sim 18.1 \times 10^{-12}\,\mathrm{m\,V^{-1}}$). In accordance to our previous investigations on waveguide embedded Bragg gratings, an increased grating strength significantly reduces the power transmission, while the modulation of both refractive index and nonlinear coefficient increases. The presented LiQPM waveguides and particularly the grating strength are carefully optimized with respect to high power transmission, mode characteristics of extraordinary polarized light at the fundamental and second harmonic frequency, and SHG conversion efficiency. The propagation loss coefficients of a pristine reference waveguide fabricated with equal parameters on the same sample are $\alpha_{\omega} = 2.88\,\mathrm{dB\,cm^{-1}}$ and

$\alpha_{2\omega} = 5.34\,\mathrm{dB\,cm^{-1}}$. Direct comparison to the presented LiQPM structure yields an absolute increase of approximately 5 dB for the fundamental and 7.5 dB for the SH due to the multiscan grating. The presented results are in good agreement with Thomas *et al.*, who achieved slightly higher modulation depth of $v = 0.82$ albeit connected to higher propagation losses of $\alpha_{\omega} = 16.4\,\mathrm{dB\,cm^{-1}}$ and $\alpha_{2\omega} = 24.5\,\mathrm{dB\,cm^{-1}}$ of the volume structured x-cut lithium niobate.[20]

Waveguide SHG in general is very sensitive to small perturbations regarding either the QPM period or waveguide properties that in turn modify the phase-matching condition.[10] The asymmetric tails of the temperature tuning curve cf. Fig. 2(a) thus can be explained by experimental constraints regarding random period errors or most importantly long term stability of the writing laser system that affect the two-dimensional refractive index profile of the waveguide and the LiQPM grating strength. Although these parameters could in principle be considered in the numerical calculation, they are neglected in this case since the associated parameter space is large and the physical quantities cannot be deduced explicitly. The induced modulation of the nonlinearity by femtosecond material processing is related to a refractive index modulation, which also affects the phase-matching condition and effective mode indices. Since the dispersion of this additional modulation is unknown, it is also neglected in the numerical calculations. A deeper understanding and investigations on the underlying changes imposed to the crystal structure for instance by nonlinear microscopy or Raman spectroscopic methods might lead to further optimized LiQPM devices.[25,26]

To demonstrate the flexibility of the direct laser writing approach and to emphasize application prospects for multi-wavelength on-chip SHG, a series of five individual LiQPM waveguides with different periods have been fabricated on a single substrate as shown in Fig. 4. The QPM period of the 8 mm long gratings is stepwise reduced by 30 nm starting at $\Lambda_1 = 6.76\,\mu\mathrm{m}$. Accordingly, the phase matching temperature shifts by approximately 15.8 °C per step, and the individual maxima are clearly separated. The LiQPM waveguide with a period of $\Lambda_4 = 6.67\,\mu\mathrm{m}$ was damaged during probe experiments with too high power and is therefore left out.

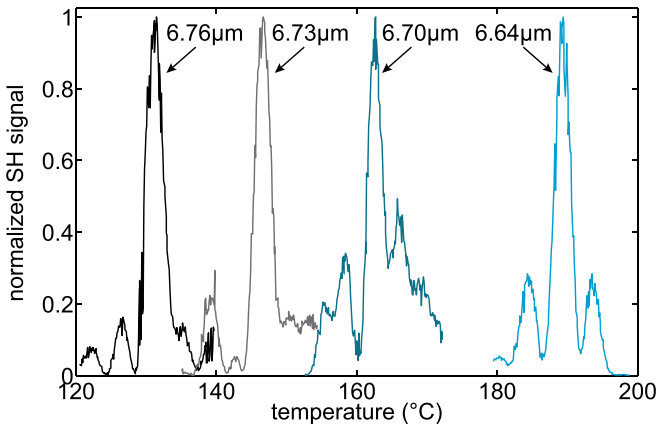

FIG. 4. Normalized temperature tuning of a series of four individual LiQPM waveguides with different grating periods. The individual waveguides with a diameter of 15 μm are inscribed with 150 nJ, while 68 nJ is used for the 8 mm long LiQPM grating section.

However, the individual SHG tuning curves demonstrate the possibility to on-the-fly engineer the interrelated quasi phase-matching temperature and second harmonic wavelength by the presented approach. In a next step, sequential stacking of LiQPM gratings in a single device for cascaded processes and multi-wavelength SHG will be possible.

It has been shown that, similar to their conventionally fabricated PPLN counterparts, the LiQPM waveguide structures possess typical narrow temperature acceptance and power dependency of the SHG process. They provide specific features of direct inscription such as high flexibility, packaging density, and compatibility to integrated optical circuits. Complex grating functions such as chirped or aperiodic sequences with sub-micron QPM gratings can be easily realized without any need for specific lithographic masks.[27,28] Moreover, the possibility to apply this technique to x-cut lithium niobate substrates enables features based on electro-optic tuning by narrow spaces integrated electrodes, which could be used for quantum optical devices.[29]

In summary, we have demonstrated monolithic fabrication of laser-induced quasi phase-matching waveguides in lithium niobate. The proposed design combines high fidelity two-dimensional waveguides and nonlinear functionality for second harmonic generation. A normalized conversion efficiency of $\eta_{norm} = 0.0637\,\%\,\mathrm{W^{-1}\,cm^{-2}}$ is achieved and multiple phase-matching temperatures equivalent to different operating wavelength are demonstrated. Due to the direct compatibility to $LiNbO_3$ integrated optics and the huge flexibility to realize complex QPM grating sequences and SHG processes, the presented LiQPM waveguides open far-reaching prospects for advanced all-integrated nonlinear devices.

[1]W. Kozlovsky, C. Nabors, and R. Byer, IEEE J. Quantum Electron. **24**, 913 (1988).
[2]M. Iwai, T. Yoshino, S. Yamaguchi, M. Imaeda, N. Pavel, I. Shoji, and T. Taira, Appl. Phys. Lett. **83**, 3659 (2003).
[3]B. Chen, C. Xu, B. Zhou, and X. Tang, IEEE J. Sel. Top. Quantum Electron. **8**, 675 (2002).
[4]B. Chen and C.-Q. Xu, IEEE J. Quantum Electron. **40**, 256 (2004).
[5]M. Saleh, G. Di Giuseppe, B. Saleh, and M. Teich, IEEE Photonics J. **2**, 736 (2010).
[6]H. Guillet de Chatellus, A. V. Sergienko, B. E. A. Saleh, M. C. Teich, and G. Di Giuseppe, Opt. Express **14**, 10060 (2006).
[7]H. J. Lee, H. Kim, M. Cha, and H. S. Moon, Appl. Phys. B **108**, 585 (2012).
[8]R. S. Weis and T. K. Gaylord, Appl. Phys. A **37**, 191 (1985).
[9]J. A. Armstrong, N. Bloembergen, J. Ducuing, and P. S. Pershan, Phys. Rev. **127**, 1918 (1962).
[10]M. Fejer, G. Magel, D. H. Jundt, and R. Byer, IEEE J. Quantum Electron. **28**, 2631 (1992).
[11]R. R. Gattass and E. Mazur, Nat. Photonics **2**, 219 (2008).
[12]G. Della Valle, R. Osellame, and P. Laporta, J. Opt. A: Pure Appl. Opt. **11**, 013001 (2009).
[13]F. Chen and J. R. V. de Aldana, Laser Photonics Rev. **8**, 251 (2014).
[14]J. Burghoff, C. Grebing, S. Nolte, and A. Tünnermann, Appl. Phys. Lett. **89**, 081108 (2006).
[15]Y. L. Lee, N. E. Yu, C. Jung, B.-A. Yu, I.-B. Sohn, S.-C. Choi, Y.-C. Noh, D.-K. Ko, W.-S. Yang, H.-M. Lee, W.-K. Kim, and H.-Y. Lee, Appl. Phys. Lett. **89**, 171103 (2006).
[16]J. Thomas, M. Heinrich, J. Burghoff, S. Nolte, A. Ancona, and A. Tünnermann, Appl. Phys. Lett. **91**, 151108 (2007).
[17]R. Osellame, M. Lobino, N. Chiodo, M. Marangoni, G. Cerullo, R. Ramponi, H. T. Bookey, R. R. Thomson, N. D. Psaila, and A. K. Kar, Appl. Phys. Lett. **90**, 241107 (2007).
[18]R. He, Q. An, Y. Jia, G. R. Castillo-Vega, J. R. Vzquez de Aldana, and F. Chen, Opt. Mater. Express **3**, 1378 (2013).

[19]S. Kroesen, W. Horn, J. Imbrock, and C. Denz, Opt. Express **22**, 23339 (2014).
[20]J. Thomas, V. Hilbert, R. Geiss, T. Pertsch, A. Tünnermann, and S. Nolte, Laser Photonics Rev. **7**, L17 (2013).
[21]J. Burghoff, H. Hartung, S. Nolte, and A. Tünnermann, Appl. Phys. A **86**, 165 (2006).
[22]W. Horn, S. Kroesen, J. Herrmann, J. Imbrock, and C. Denz, Opt. Express **20**, 26922 (2012).
[23]S. Gross, M. Ams, D. G. Lancaster, T. M. Monro, A. Fuerbach, and M. J. Withford, Opt. Lett. **37**, 3999 (2012).
[24]N. Umemura, D. Matsuda, T. Mizuno, and K. Kato, Appl. Opt. **53**, 5726 (2014).
[25]Y. Sheng, A. Best, H.-J. Butt, W. Krolikowski, A. Arie, and K. Koynov, Opt. Express **18**, 16539 (2010).
[26]A. Rodenas, A. H. Nejadmalayeri, D. Jaque, and P. Herman, Opt. Express **16**, 13979 (2008).
[27]M. A. Arbore, A. Galvanauskas, D. Harter, M. H. Chou, and M. M. Fejer, Opt. Lett. **22**, 1341 (1997).
[28]G. K. Kitaeva, Phys. Rev. A **76**, 043841 (2007).
[29]Y. Ming, A.-H. Tan, Z.-J. Wu, Z.-X. Chen, F. Xu, and Y.-Q. Lu, Sci. Rep. **4**, 4812 (2014).